JOURNAL OF AIRCRAFT
Vol. 33, No. 5, September–October 1996

Time-Dependent Supersonic Separation of Tangent Bodies

Neal A. Mosbarger*
U.S. Air Force Wright Laboratory, Wright–Patterson Air Force Base, Ohio 45433-7936
and
Paul I. King†
U.S. Air Force Institute of Technology, Wright–Patterson Air Force Base, Ohio 45433-7936

An experimental, time-dependent separation of tangent bodies was performed in a supersonic wind tunnel (Mach 1.5 and 1.9) to investigate the significance of transient effects and the suitability of using steady-state assumptions to predict a dynamic separation event. Model configurations consisted of two bodies placed in a near tangent position. A stationary body, a plate or ogive, was instrumented to obtain dynamic surface pressures, while a second body, a wedge attached to an air cylinder, was plunged in a constrained motion away from and toward the stationary model. Three-dimensional flow expansion around the edge of the wedge reduced the strength of incident shock waves and created a region of low pressure, near freestream static, on body surfaces between the incident and reflection shock waves. Dynamic motion of the wedge did not significantly affect shock-wave development between the bodies, and steady-state corrections that accounted for the motion-induced wedge angle were appropriate for predicting time-dependent surface pressures induced by the incident shock wave. However, unsteady pressures caused from the motion of the wedge were evident when separation distances were less than 20% of the wedge width.

Nomenclature

D = wedge-store width, 6.35 cm
M = Mach number
P = surface pressure normalized by freestream static pressure
P_∞ = freestream static pressure, N/m^2
t = time, s
V = flow velocity, m/s
v = store velocity, m/s
X = axial distance, cm
X_{LE} = distance downstream of leading edge normalized by plate length, 20.3 cm
X/YE = axial distance normalized by ogive maximum radius, 1.91 cm
Y = separation distance between wedge-store and stationary model, cm
Y/D = normalized separation distance
YE = ogive maximum radius, 1.91 cm
Z = plate span distance normalized by plate width, 20.3 cm
α_e = effective AOA or effective wedge angle, deg
α_u = induced AOA or induced wedge angle, deg
β = shock-wave angle, deg
γ = specific heat ratio
ε = geometric AOA or geometric wedge angle, deg
ρ = density, kg/m^3
ϕ = transducer orientation on plate, deg
ψ = transducer orientation on ogive, deg

Subscripts
c = closure motion
s = separation motion
1 = upstream of shock wave
2 = downstream of shock wave
∞ = freestream

Introduction

SUPERSONIC flow around an integrated aircraft with an externally mounted store is complex, involving viscous flow, shock waves, and mutual aerodynamic interference. An understanding of the initial store separation phase is complicated by the time dependency of the dynamic event. Before computational fluid dynamic (CFD) advances in time-dependent simulation (e.g., dynamic and chimera grids), store trajectory prediction methods were simplified with steady-state assumptions. Since the relative velocity of the store is significantly less than freestream velocity, it was assumed that for a given store position time dependency could be accounted for by adding an induced AOA [$\alpha_u = \arctan(v/V_\infty)$] into the steady-state calculations. (A steady-state assumption implies that the flow is instantaneously developed for each store position during a store separation event.) However, until this investigation, the steady-state assumption had not been tested experimentally, particularly for the initial separation phase of tangent bodies. This lack of experimental verification has been a concern since numerical comparisons of steady-state and time-dependent separation simulations indicate differences in the store aerodynamic coefficients and flowfield characteristics.[1] Thus, one objective of this study was to quantify the differences between steady-state and time-dependent separations of tangent bodies in a supersonic flow.

Trajectory predictions dependent upon steady-state aerodynamic coefficients have correlated well with some flight tests. However, when problems do arise in flight test the most common cause is underpredicted store rotation rates.[2] Since the store trajectory is sensitive to initial conditions, improvements in the determination of dynamic effects on the store during the initial separation phase would increase the accuracy of the trajectory predictions. Recent developments in CFD have addressed the initial time-dependent conditions with some success.[3–6] However, there are disconcerting differences found between steady-state and time-dependent numerical solutions for equivalent store separation simulations. Both Belk et al.[7] and Meakin's[8] CFD simulations showed that near the shock

Received June 15, 1995; revision received June 3, 1996; accepted for publication June 4, 1996.

*Captain, Aeromechanics Division.
†Associate Professor, Department of Aeronautics and Astronautics.

waves, time-dependent values (pressure and aerodynamic coefficients) were reduced in magnitude and lagged in phase (location of the shock wave) compared to the equivalent steady-state solution. The solutions are disconcerting because they raise doubts about the validity of the current and popular use of steady-state experimental techniques to characterize the time-dependent separation events.

Background

One desirable wind-tunnel test would be an experimental duplication of the Belk et al.[7] time-dependent numerical simulation, where the moving stores are impulsively started and maintained at an equivalent effective AOA, yielding a clear identification of the unsteady effects. Unfortunately, there is no physical step function that can be applied to the store to give it an instantaneous constant velocity. Although each separation event can have the same geometric AOA ε (relative position with respect to the freestream), the induced AOA $\alpha_u = \arctan(v/V_\infty)$, and therefore, the effective AOA α_e, will change with the varying v, since

$$\alpha_e = \varepsilon + \alpha_u \tag{1}$$

Shock-Wave Perturbation Predictions

Downstream of a three-dimensional curved shock wave the flow exhibits complex, rotational characteristics and a nonuniform entropy distribution.[9] This type of flow is governed by nonlinear differential equations that can only be solved with numerical techniques. Although a completely analytical solution for the flow downstream of a three-dimensional shock wave is not possible, an estimation of the flowfield parameters may be made for a small change in the shock-wave strength (perturbation), if the initial solution is known. Since the investigation was directed toward differences between separation events, certain assumptions were introduced to allow a simplified perturbations approach for predicting the shock-induced pressure profiles. These assumptions were as follows:

1) The first-order perturbation to the flowfield occurs in the store plane of motion. The moving wedge-store primarily deflects the flow two dimensionally. The perturbed velocity is parallel to the wedge motion, changing the induced AOA and the attached shock-wave angle and strength.

2) The shock wave attached to the wedge store has the characteristics of a two-dimensional shock wave for most of the wedge width near the wedge surface and for a distance between the wedge store and plate not to exceed the wedge width. The intersection of the wedge-store motion plane, that which includes the wedge-store axial centerline and the attached shock wave, is nearly a straight line.

The primary effect induced by a moving wedge store is the change in strength and angle of the attached shock wave. These assumptions limit the flow perturbations to a plane across a nearly straight shock wave. A preliminary review of the data indicated a two-dimensional approach would be appropriate, most particularly for the configuration symmetry plane. Thus, it is assumed that the store motion introduces an irrotational perturbation into a rotational flowfield downstream of the attached shock wave. The characteristics of the perturbed attached shock wave may be divided into two components: 1) position and 2) strength of the shock wave.

Equipment

Wind Tunnel

The experiment was conducted in the 0.61 × 0.61 m (2 × 2 ft) test section of the Trisonic Gasdynamic Facility (TGF) located at Wright–Patterson AFB, Ohio. The TGF is a closed-circuit, variable-density, continuous flow wind tunnel capable of operating at subsonic, transonic, and supersonic velocities.[10] Freestream supersonic velocities are obtained with fixed area-ratio nozzles that result in Mach numbers of 1.52 and 1.91. At Mach 1.52 the Reynolds number per meter is $0.64 \times 10^{+6}$. At Mach 1.91 the Reynolds number per meter is $0.55 \times 10^{+6}$.

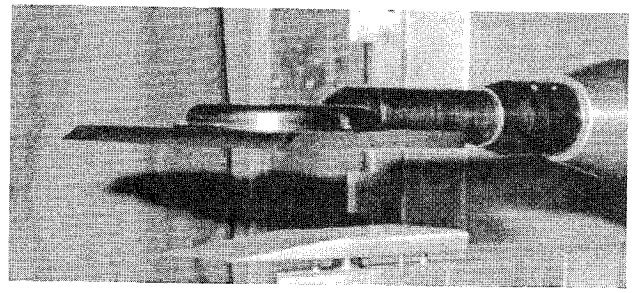

Fig. 1 Plate and wedge-store configuration.

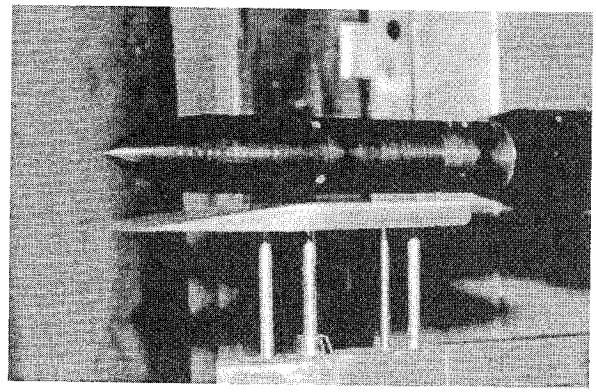

Fig. 2 Ogive and wedge-store configuration.

Experimental Models

Two models were tested: 1) a fixed flat plate positioned near a moving 6.1 or 3.5 deg (upper half angle) wedge-shaped store as shown in Fig. 1 and 2) a fixed ogive positioned near a moving wedge-shaped store (Fig. 2). In all configurations, the fixed models were mounted on a central stationary sting and instrumented to measure dynamic surface pressures. The separating store was connected to a two-way air cylinder and a linear variable differential transformer (LVDT) located in a housing assembly mounted to the tunnel floor.

Experimental Method

The experimental approach in this work involved two bodies placed in a near tangent position and dynamically separated in a constrained motion. The wedge store was attached to an air cylinder and impulsively plunged in a predetermined vertical motion away from (separation) or toward (closure) the stationary model similar to Belk's et al.[7] numerical simulation of a reflection plate and a parabolic store. The plate and wedge configuration (Fig. 1) simulated a wing and store separation. The ogive and wedge store (Fig. 2) was used to investigate the movement of an oblique shock wave intersecting a conical-shaped shock wave. The time-dependent surface pressures associated with the shock-wave pattern between the two bodies were measured on the stationary body during the dynamic motion of the wedge store. Steady-state measurements, made with the wedge store at a fixed position, were used to evaluate the basic flow characteristics between the two bodies. Analysis of the time-dependent experimental data was used to evaluate the accuracy of steady-state assumptions in predicting time-dependent influences of the moving wedge store.

Steady-State Data Reduction

The mean pressure was determined for steady-state store separation positions using the subroutines from *Numerical Recipes*.[11] The mean of $x_1, \ldots, x_N$ is defined as

$$\bar{x} = \frac{1}{N} \sum_{j=1}^{N} x_j \tag{2}$$

A nominal one-thousand samples were collected with an acquisition rate of 50 kHz for each steady-state position (chosen for convenience to match the time-dependent data sample rate).

Dynamic Separation Data Reduction

Each dynamic separation run was repeated a minimum of five times, i.e., five closures or five separations. Surface pressures were obtained on the stationary model at each *Y/D*, the distance between the plate-sensing surface (or the cylindrical portion of the ogive) and the shoulder of the separating wedge store divided by the wedge width, $D = 6.35$ cm. For a single-store motion, the pressure at any *Y/D* was obtained from the simple average of pressures at nondimensional positions *Y/D* $= \pm 0.0005$ about the *Y/D* of interest. The ensemble mean pressure ($N = 5$) is defined as

$$\bar{x}\left(\frac{Y}{D}\right) = \frac{1}{N}\sum_{j=1}^{N} x_j\left(\frac{Y}{D}\right) \tag{3}$$

Wedge-Store Velocity

At each time-dependent separation position $Y(t_1)$, the average wedge-store velocity was calculated with a simple central difference quotient ($\Delta Y/\Delta t$). An acquisition rate of 50 kHz was chosen so that at a nominal wedge-store velocity of 1.8-m/s data would be acquired for intervals of 0.1 mm, which exceeds the resolution of the LVDT (0.07 mm).

Shock-Wave Impingement

Experimentally, a different α_e occurs for the time-dependent separation and closure motions of the wedge store. The data for the wedge store moving toward the plate (closure) were arbitrarily chosen as the reference data set. The data set associated with separation was perturbed (adjusted to account for a small change in α_e) to predict the closure data set. The difference between the closure and the perturbed separation data set (closure prediction) will aid in the identification of unsteady effects associated with the tangent separation of the wedge store and plate.

Prediction of the shock-wave impingement location on the plate surface during closure motion was determined by perturbing the separation data set such that the closure prediction and closure data sets had the same α_e. Determination of α_e [Eq. (1)] for each time-dependent event depended only on α_u, since ε remained fixed. With α_e determined for each time-dependent event, the β can be calculated from two-dimensional shock-wave theory. The shock-wave impingement location on the plate surface (X_{LE}) varies with wedge-store position and was determined assuming a straight shock wave as shown in Fig. 3, also verified with schlieren photographs,[12] attached to the wedge vertex at a given separation position.

Since the pressure history was available only at fixed surface locations, it was convenient to predict the particular wedge-store separation position needed for the attached shock wave to impinge at any X_{LE}. Setting X_{LE} for the separation and closure events equal for the corresponding Y_s position during separation, a closure position Y_c can be calculated using the linear equation, $X = Y \times m + b$ (where m and b are, respectively, the slope and Y-axis intercept of the shock impingement location and wedge position linear relationship), resulting in

$$Y_c = \frac{Y_s m_s + b_s - b_c}{m_c} \tag{4}$$

With closure distances calculated from Eq. (4), discrepancy between predicted and experimental time-dependent results are henceforth defined as the transient effects.

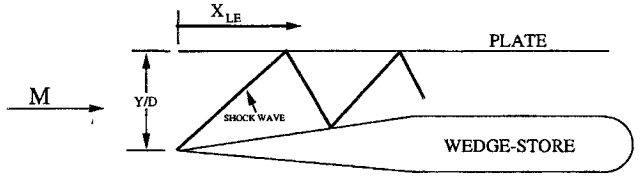

Fig. 3 Diagram of the shock wave between the wedge store and plate.

Pressure Prediction

The pressure rise across a shock wave can be determined from two-dimensional shock-wave relationships[13]

$$\frac{P_2}{P_1} = \frac{2\gamma}{\gamma + 1} M_{1n}^2 - \frac{\gamma - 1}{\gamma + 1} \tag{5}$$

The prediction of the plate surface pressure associated with the wedge-store closure motion was made by adding to the experimental separation surface pressure the difference between the calculated pressure rises [Eq. (5)] for the separation and closure events. Since the upstream Mach number is the same for separation and closure, the normalized upstream pressure must also be equivalent. Therefore, the pressure downstream of the attached shock wave for closure may be predicted (P_{2p}) from the separation data (P_{2s}) and the calculated pressure difference between separation and closure events:

$$P_{2p} = P_1 \Delta \frac{P_2}{P_1} + P_{2s} \tag{6}$$

The flow at the surface of the stationary model must pass through the oblique shock-wave impingement (incident and reflection shock). Furthermore, the incident shock-wave strength is reduced by the three-dimensional flow induced by the finite wedge-store width. Therefore, there is some uncertainty as to what the total surface pressure change will be after the passage of the impinging shock wave. Despite the fact that experimental and numerical surface pressures do not conform to two-dimensional analysis, the attached shock wave remains nearly planar as discussed in the Results and Discussion section, particularly for the close proximity of the wedge-store and plate ($Y/D \leq 0.89$). Thus, discrepancies between predicted and experimental results of the shock-wave location will be the primary indicator for identifying the transient effects, and the comparison of predicted and experimental surface pressure values will be used for reference purposes to evaluate the potential magnitude of the transient pressures.

Results and Discussion

Steady-State Events

Steady-state experimental and numerical results indicated three-dimensional flow characteristics downstream of the initial shock wave attached to the wedge-store vertex. Since the wedge store was of a finite width, the flow expanded into the spanwise region off the edge of the wedge store where the pressure was lower, and resulted in regions of nonuniform flow deflections, low shock-induced surface pressures, decreasing pressures, and curving shock waves.

For comparison, a two-dimensional flow of Mach 1.52 encountering a 6.1-deg wedge has a normalized pressure jump (P_2/P_∞) across the initial shock wave of 1.35. At the plate, where the wedge-induced shock wave impinges, the flow crosses the shock wave reflecting off the plate surface and maintains a flow parallel to the plate surface, with a total pressure ratio (P_3/P_∞) of 1.91.

The general features of the shocks and expansions for the aforementioned example are reproduced from experimental data in Fig. 4. With the wedge store at $Y/D = 0.51$, a pressure

peak of only 1.50 occurred near $X_{LE} = 0.34$. A three-dimensional inviscid (Euler) simulation showed that the three-dimensional expansion region downstream of the initial shock wave was responsible for the low experimental pressures. In Fig. 5 the magnitude of the normalized pressure peak induced by the initial shock wave is slightly higher (1.57) than the experimental pressure peak (1.50), but is still significantly less than the analytical two-dimensional predicted value (1.91). Overall, plate surface pressures were well predicted by the three-dimensional Euler simulation.

The pressure troughs downstream of the shock waves were a significant characteristic of the flowfield between the wedge store and stationary models. Contrary to the expected rise in surface pressure through a shock-wave reflection pattern, the experimental surface pressure results (Fig. 4) reveal a flow expansion, to near freestream conditions at the plate centerline, between the impinging initial and reflection shock waves ($P = 1.0$ at $X_{LE} = 0.45$). The numerical surface pressure results for the plate (Fig. 5) also show a pressure trough near $X_{LE} = 0.59$ that extends in the streamwise and spanwise direction from the plate centerline to the intersection of the initial curving shock wave near $X_{LE} = 0.79$ and $Z = 0.59$. The three-dimensional flow expansion not only created a low-pressure region on the plate surface, but also created regions of low pressure in the flowfield between the bodies and on the surface of the wedge store.

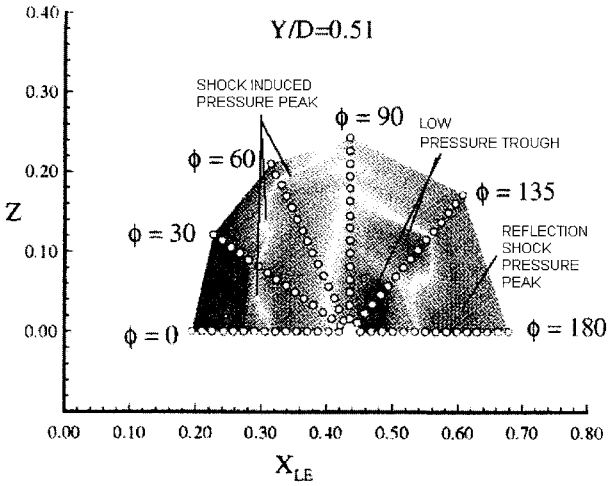

Fig. 4 Plate experimental pressure contour: $M = 1.52$, 6.1-deg wedge, $Y/D = 0.51$.

Numerical results showed that the flow expansion downstream of the shock wave also reduced the wedge-store surface pressures to a freestream value, as seen in Fig. 6. Immediately downstream of the vertex ($X_{LE} = 0.18$, $Z \leq 0.16$), the surface pressure rises to the two-dimensional predicted value ($P = 1.35$) as it crosses the attached shock wave. The decrease in pressure begins at $X_{LE} = 0.21$ near the edge of the wedge ($Z = 0.16$) and reaches a near freestream condition along the wedge-store centerline ($Z = 0.0$) at $X_{LE} = 0.44$.

These regions of flow expansion between the separating bodies are an unfavorable condition for stores having pitch-up tendency[14] and conformal-shaped stores designed to reduce aerodynamic drag and radar signature. The three-dimensional flow expansion also complicates the analysis of a wedge store separating from a stationary body. An analysis of wedge-store separation using oblique, two-dimensional shock-wave relationships would predict a Mach disk downstream of the initial shock impingement for the previous case. Incorporating an artificial two-dimensional expansion (Prandtl–Meyer flow) into the analysis is not any better, since doing so allows the flow

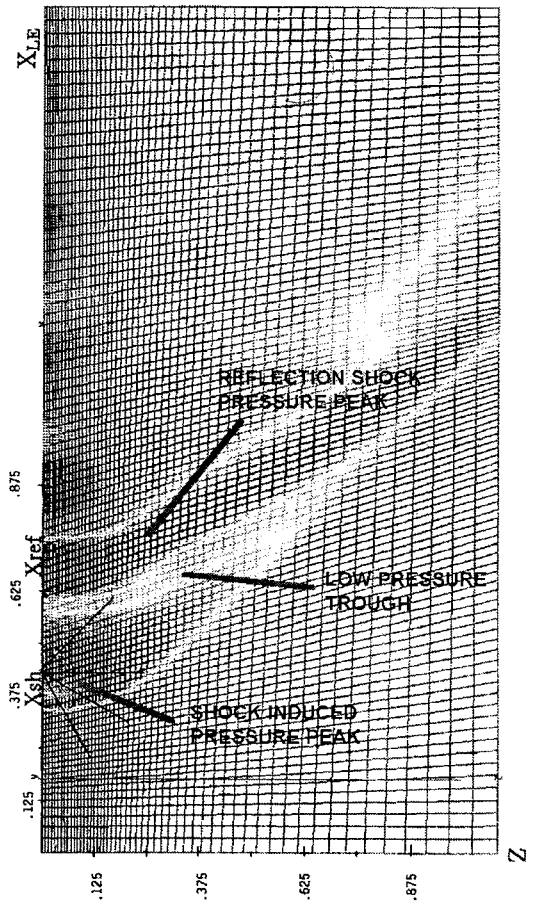

Fig. 5 Plate numerical surface pressure: $M = 1.52$, 6.1-deg wedge, $Y/D = 0.51$.

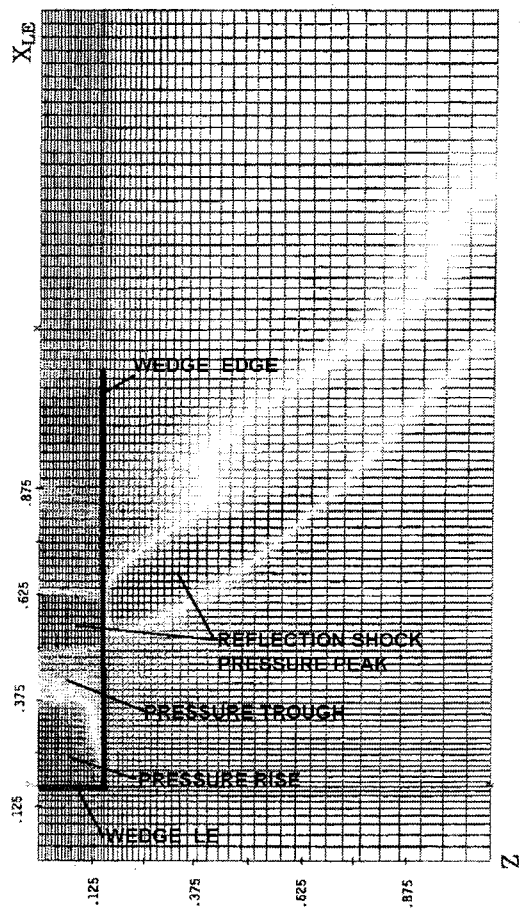

Fig. 6 6.1-deg wedge numerical surface pressure, $M = 1.52$.

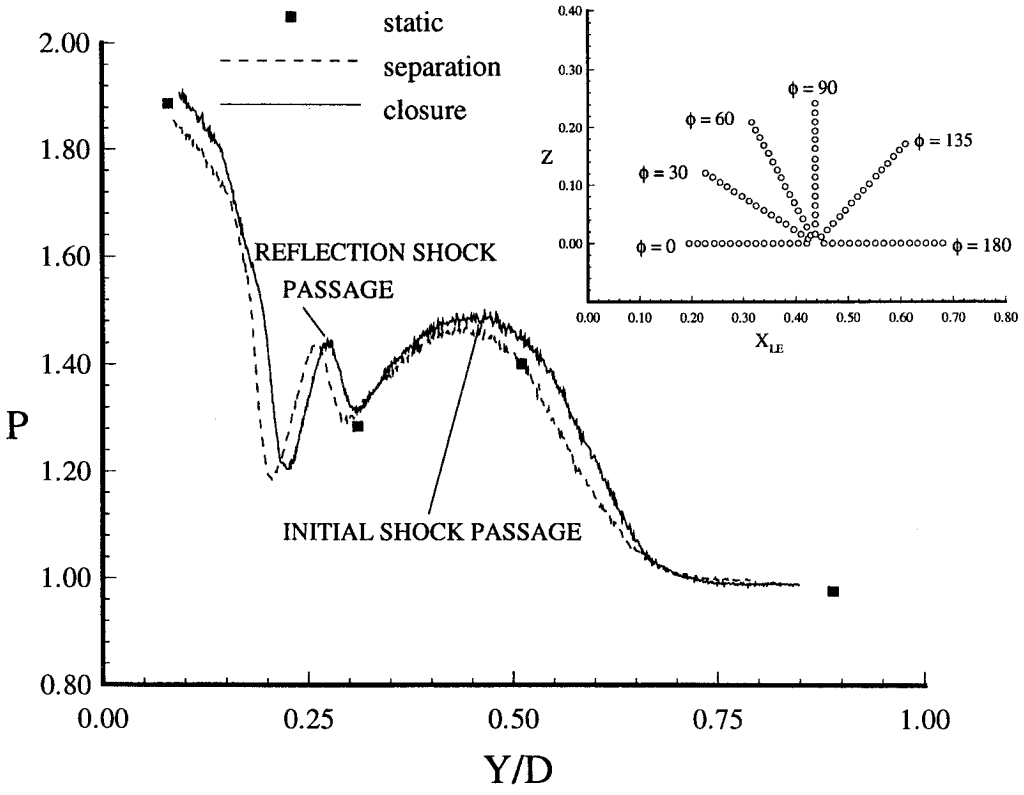

Fig. 7 Normalized plate surface pressure for dynamic motion with 6.1-deg wedge and M = 1.52 (ϕ = 0, X_{LE} = 0.32).

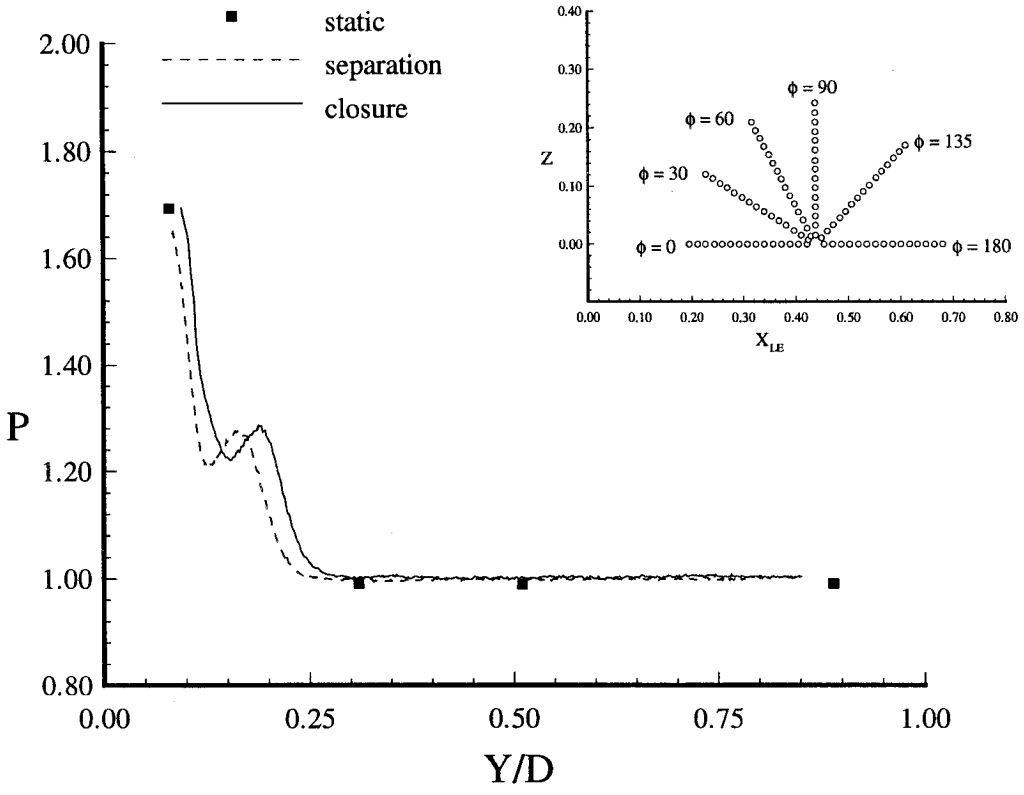

Fig. 8 Normalized plate surface pressure for dynamic motion with 6.1-deg wedge and M = 1.52 (ϕ = 30 deg, X_{LE} = 0.24, Z = 0.11).

to become overexpanded compared to experimental or three-dimensional numerical results.

Time-Dependent Event: Plate and Moving Wedge

A typical separation event included movement of the wedge store 4.24 cm in 26 ms, an average speed of 1.6 m/s, and a maximum $\alpha_u = -0.0051$ rad for a freestream Mach number of 1.52. For closure, a distance of 4.88 cm was covered in 27 ms at an average speed of 1.8 m/s and reached a maximum $\alpha_u = 0.0057$ rad (M = 1.52).

The differences between two time-dependent (separation and closure) pressure results are because of differences in the ef-

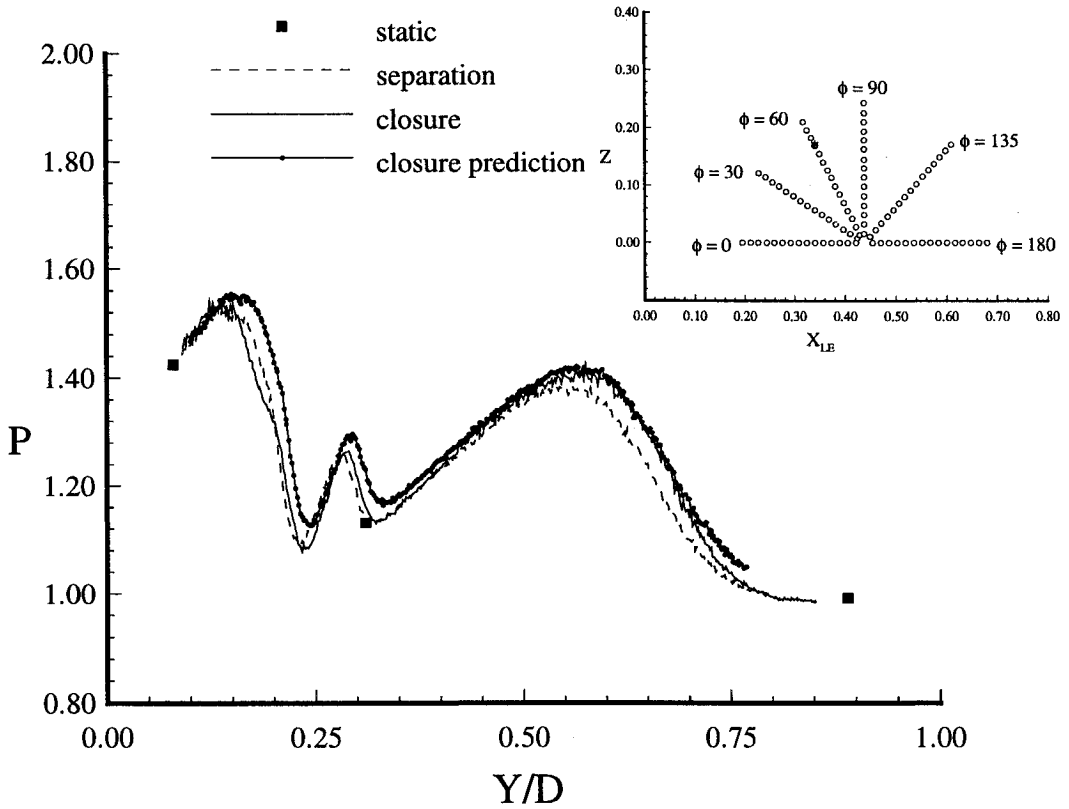

Fig. 9 Normalized plate surface pressure for dynamic motion with 6.1-deg wedge and $M = 1.52$ ($\phi = 60$ deg, $X_{LE} = 0.34$, $Z = 0.17$).

fective angle α_e. An increase in the effective wedge angle ($\alpha_e = \alpha_u + \varepsilon$) for closure at a constant Mach number produces an increase in the shock-wave strength and β. Since the wedge store must be at a greater Y/D distance than in the separation event for an initial shock impingement at the same location on the plate (X_{LE}), the closure event lags the separation event, as indicated by surface pressures in Fig. 7.

The combination of two local peaks and troughs in Fig. 7 indicates the development of a shock-wave reflection pattern between the two bodies. With the wedge store at the fully separated steady-state position ($Y/D = 0.89$), the initial shock wave impinges downstream of $X_{LE} = 0.32$ (thus, $P = 1.00$). As the closure pressure profile is traced for decreasing Y/D, the initial shock wave produces a local pressure peak at $Y/D = 0.46$ with $P = 1.49$. As the initial shock wave moves further upstream because of the closing motion of the wedge store, the effect of the spanwise expansion flow causes a pressure trough at $Y/D = 0.31$. With further reductions in the separation distance, the pressure rises again because of the influence of the reflection shock off the wedge-store surface. The reflection shock creates a second peak at $Y/D = 0.27$. The pressure trough at $Y/D = 0.22$ results from the flow expansion downstream of the reflection shock. A final pressure rise occurs as the wedge-store approaches the near-touch position.

Off-axis pressure transducers on the plate surface near the region of the orthogonal projection of the wedge-store edge ($Z = 0.16$) revealed an increased flow expansion effect. For a transducer setting of $\phi = 30$ deg, the furthest upstream position to capture a shock-wave passage was at $X_{LE} = 0.24$, $Z = 0.11$. In Fig. 8, the separation distances for shock-induced pressure peaks show the closure event ($Y/D = 0.19$) lagging the separation event ($Y/D = 0.16$). Although the closure event induced a stronger shock wave than the separation event, the magnitude of the shock-induced pressure peaks was nearly equal ($P \approx 1.28$), because the flow expansion about the wedge-store edge reduced the pressure influence of the initial shock wave impingement, eliminating the expected pressure difference between the time-dependent separation and closure events.

At greater separation distances, however, the plate surface pressure was less influenced by the flow expansion about the wedge-store edge. In Fig. 9, for the pressure transducer positioned farther downstream ($X_{LE} = 0.34$, $Z = 0.17$) and closer to the projected wedge-store edge $Z = 0.16$, the differences in initial-shock-induced pressure magnitudes were not as influenced by the edge-induced flow expansion as the results shown in Fig. 8. Because of the location of the transducer, the passage of the initial shock wave on the plate surface (closure event peak pressure at $Y/D = 0.58$) occurred at a greater separation distance than for the upstream pressure transducer locations. In this case, there was a difference in the shock-induced pressure peaks ($\Delta P = 0.03$) between the separation and closure events, whereas in Fig. 8, the shock-induced pressure peaks were equal. As the separation distance decreased to the near-touch phase ($Y/D \leq 0.20$), edge effects eliminate the pressure difference between the time-dependent separation and closure events (Fig. 9).

The influence of the flow expansion about the wedge-store edge during the near-touch phase is seen in Fig. 10 for the transducers set at $\phi = 90$ deg. All transducers are at the streamwise location $X_{LE} = 0.44$, but differ on their distance from the plate centerline: $Z = 0.02$, 0.15, and 0.24. Progressing outward from the plate centerline, surface pressures decreased for $Y/D \leq 0.20$ because of the proximity of the wedge-store edge.

A correlation exists between the influence of the wedge-edge expansion flow and the range of the surface pressures downstream of the shock waves. Basically, the area of the plate most influenced by the wedge-edge expansion had a lower pressure for $Y/D \leq 0.20$ and a smaller range of pressure variation downstream of the shock waves ($Y/D \leq 0.40$). For example, in Fig. 10, at $Z = 0.24$ there was a maximum pressure of 1.41 at $Y/D = 0.10$ and a minimum pressure of 1.15 at $Y/D = 0.26$ for a range in pressure of $\Delta P = 0.26$. Near the plate centerline ($Z = 0.02$), however, the maximum pressure at $Y/D = 0.10$ was $P = 1.74$, and the minimum pressure was $P = 1.02$ at $Y/D = 0.30$ for a pressure range three times that of $Z = 0.24$ ($\Delta P = 0.72$). In other words, the flow expansion at the outboard po-

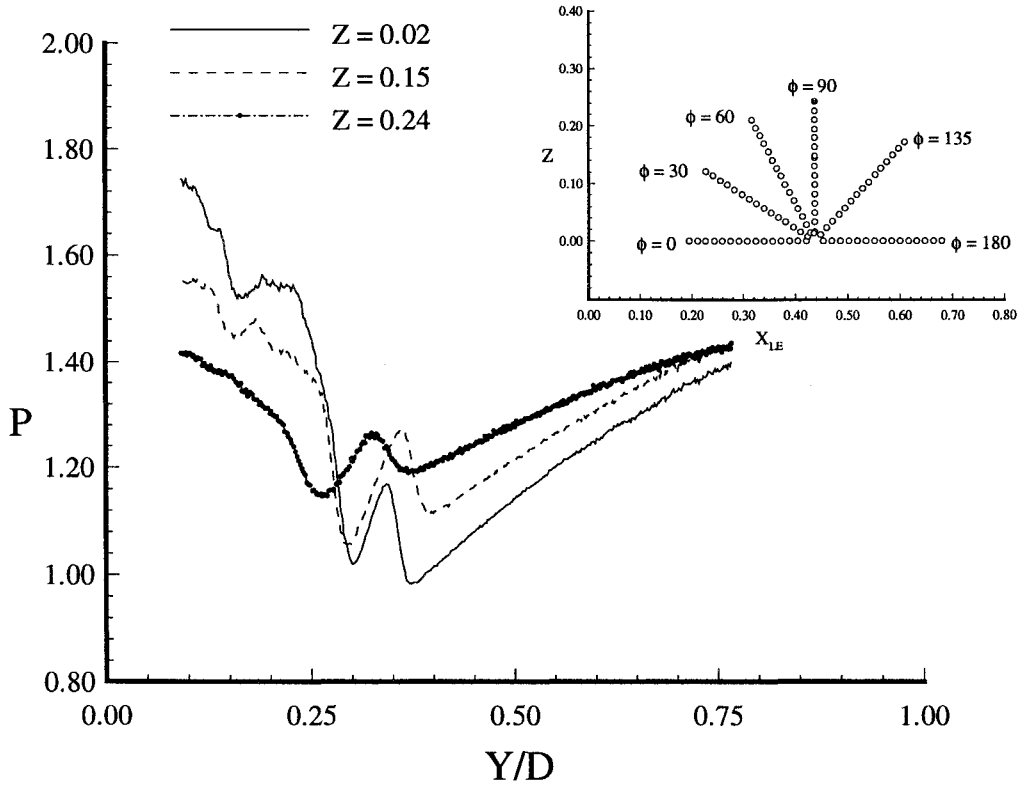

Fig. 10 Normalized plate surface pressure for dynamic motion with 6.1-deg wedge and $M = 1.52$ ($\phi = 90$ deg, $X_{LE} = 0.44$).

sitions reduces the pressure peaks and expected pressure difference between the separation and closure events caused by α_e, whereas the flow expansion inboard induces a larger pressure variation between the peak and trough within a single separation or closure event.

Expansion of the flow between the two bodies during the near-touch phase of separation had the most significant effect on the surface pressures and the greatest implications to the store separation event. The experimental results revealed that the greater the surface pressures, the stronger the flow expansion became. This characteristic of the expansion flow implies that the aircraft and store integration should strive to avoid high near-touch pressures to moderate the pressure variation at greater separation distances. Reducing the strength of the expansion flow would retard the unfavorable flow-induced pitch-up mechanism encouraged by the low-pressure region between the bodies.

Time-Dependent Event: Ogive and Moving Wedge

The ogive baseline test configuration consisted of the pressure-instrumented ogive and the 6.1 deg wedge store at freestream Mach 1.9. The leading edge of the wedge store was placed at the same streamwise position as the nose of the ogive to capture the passage of the initial shock wave within the region of the pressure transducer locations. The ogive configuration flowfield characteristics differed from that of the plate configuration in several ways. First, the initial shock wave attached to the wedge store intersected a conical-shaped shock wave induced by the ogive prior to impinging on the ogive surface. Second, the magnitude of the shock-wave-induced pressure peaks and the piston action influence were reduced on the three-dimensional ogive surface as compared to the two-dimensional surface of the plate.

The pressure profile for the ogive transducer position of $X/YE = 3.10$, $\psi = 0$ deg (Fig. 11), indicates similar spatial characteristics to those found along the plate centerline: shock-wave-induced pressure rise, flow expansions downstream of the shock waves, and piston-type responses at near-touch conditions. For the closure event, the initial shock-wave-induced pressure peak occurred at $Y/D = 0.49$. The three-dimensional flow expansion downstream of the wedge-induced shock wave resulted in a pressure reduction (trough) for separation distances of $0.31 \leq Y/D \leq 0.49$. The reflection of the conical shock wave from the wedge-store surface is indicated by the small pressure peak at $Y/D = 0.25$. Finally, a pressure plateau is apparent for $Y/D \leq 0.15$, but the pressure difference caused by the piston action for separation and closure events is small, $\Delta P = 0.03$, compared to the maximum pressure difference along the plate centerline $\Delta P \approx 0.12$, as discussed in the Prediction Results section.

At locations rotated away from the wedge store $\psi > 0$ deg, the magnitude of the shock-induced pressure peaks was reduced because of the orientation of the impinging shock wave. Whereas, for $\psi = 0$ deg, a full deflection of the flow crossing the shock wave occurred such that flow tangency to the surface of the ogive was maintained, as ψ increases, only a component of the velocity vector downstream of the impinging shock wave is directed toward the ogive surface; therefore, the deflection angle through the reflection shock wave is also reduced as is the resulting pressure increase. The pressure reduction associated with increasing ψ can be approximated using the analytical method from Yin.[15] Ignoring the conical shock wave induced by the ogive, an additional simplifying assumption, the pressure ratio for an impinging planar shock at $\psi = 30$ deg to that of $\psi = 0$ deg is 0.96. Experimental results revealed a similar value of 0.94 (at the transducer location of $X/YE = 3.64$).

There was no significant difference in surface pressure between the time-dependent separation and closure events for the transducers set at $\psi \geq 90$ deg. The pressure differences induced by the change in α_e did not propagate into ogive surface regions not impinged upon by the initial shock wave.

Prediction Results

Any time-dependent effects associated with shock-wave development can be inferred from a comparison of experimental closure data with predictions based on steady-state assumptions. The initial shock-wave-induced surface pressure for the

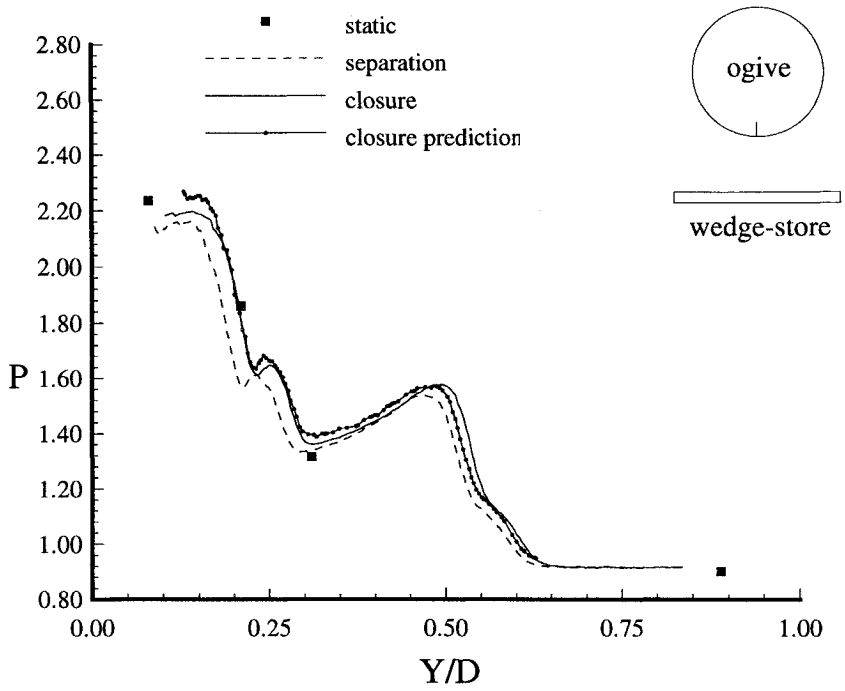

Fig. 11 Ogive surface pressure at X/YE = 3.10 and ψ = 0 deg (6.1 deg, M = 1.9).

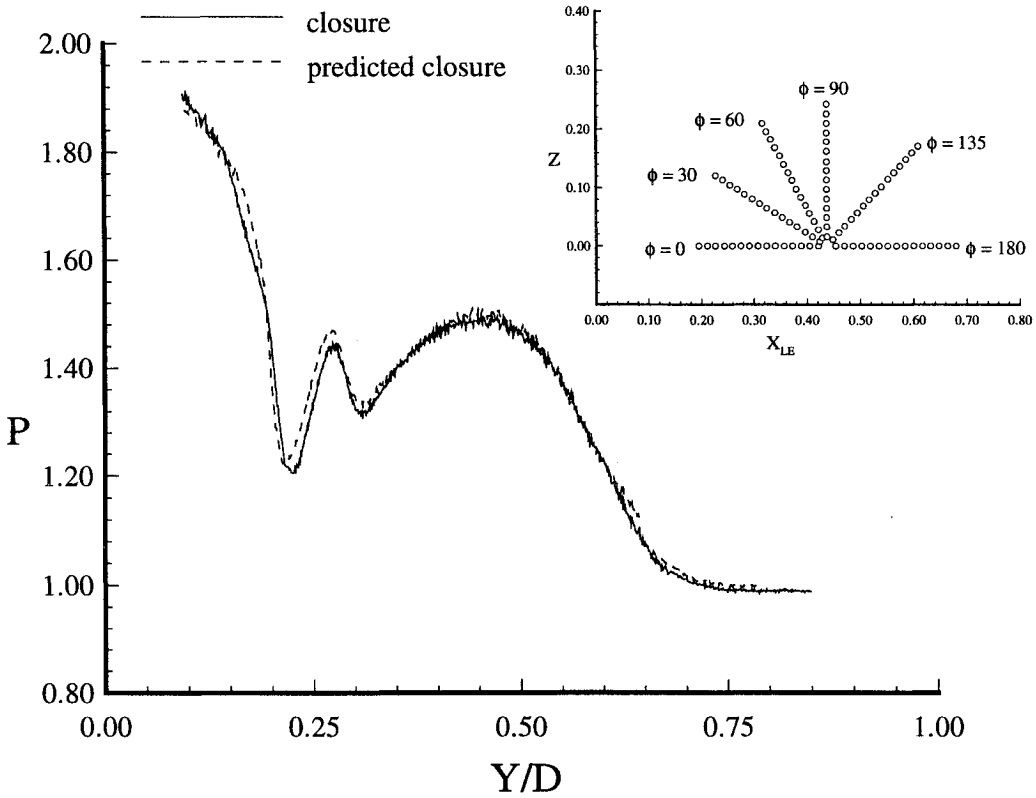

Fig. 12 Normalized plate surface pressure for dynamic motion with 6.1-deg wedge and M = 1.52 (ϕ = 0 deg, X_{LE} = 0.32).

closure event was predicted from separation data perturbed so that closure and perturbed separation events had the same α_e.[12]

Plate Configuration

The pressure influence of the initial impinging shock wave was predicted for the closure event along the plate centerline (ϕ = 0 deg). Results of the prediction method are given for X_{LE} = 0.32 with the 6.1 deg (Fig. 12) and the 3.5 deg (Fig. 13) wedge-store configurations. In Figs. 12 and 13, the closure event pressures from the upstream influence position of $Y/D \approx 0.60$ through the pressure peaks at Y/D = 0.45 for the 6.1-deg wedge store (Fig. 12) and at Y/D = 0.50 for the 3.5-deg wedge store (Fig. 13), show a good agreement of the prediction method with the closure data. Since only steady-state assumptions were used to predict the closure event, the match between prediction and closure leads to the conclusion that no significant time-dependent shock-wave-induced pressures are associated with the movement of the wedge store.

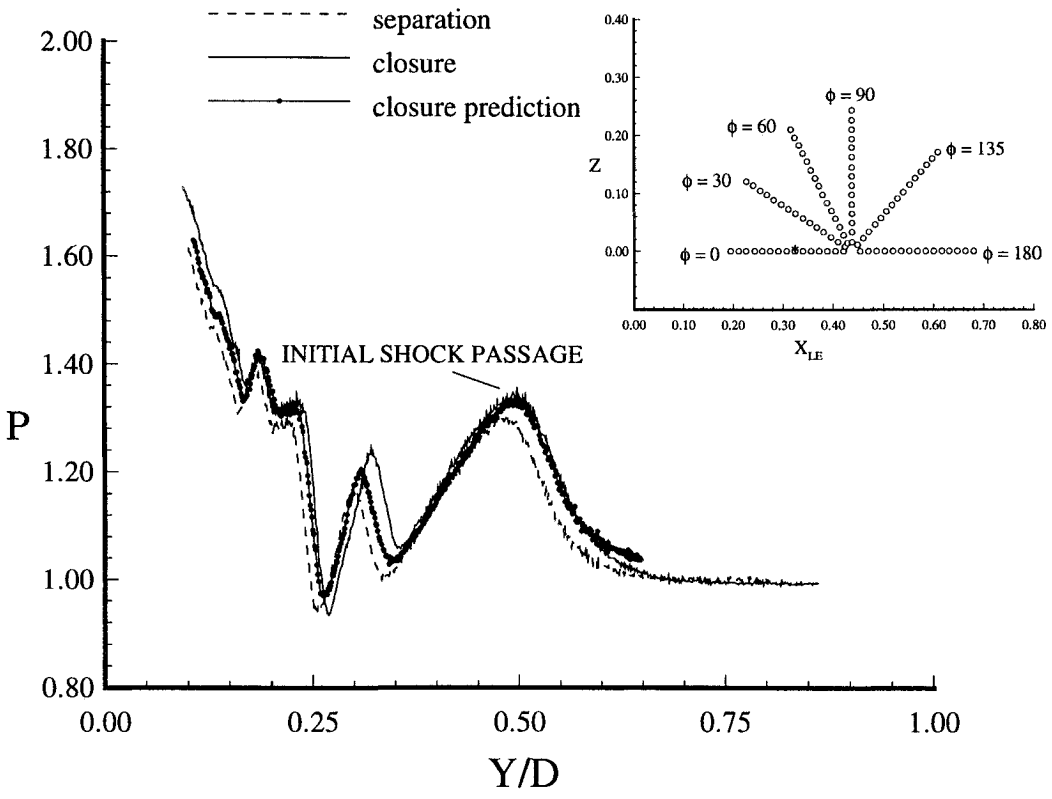

Fig. 13 Normalized plate surface pressure for dynamic motion with 3.5-deg wedge and M = 1.52 (ϕ = 0 deg, X_{LE} = 0.32).

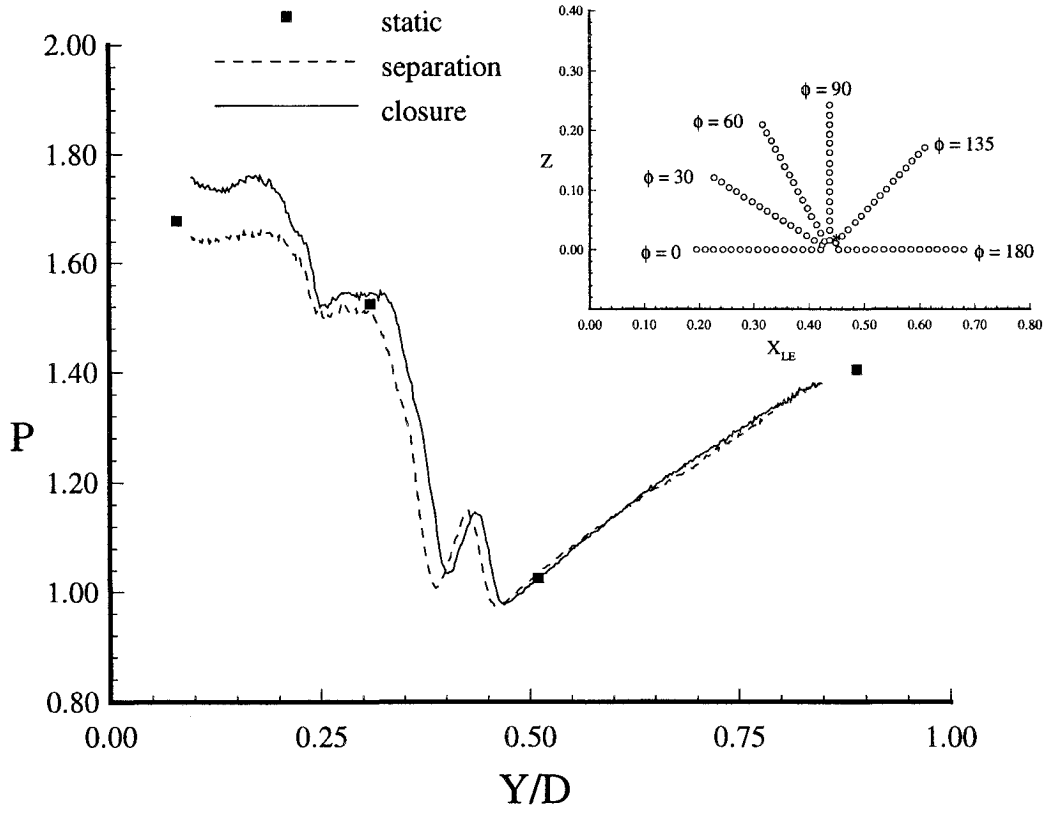

Fig. 14 Normalized plate surface pressure for dynamic motion with 6.1-deg wedge and M = 1.52 (ϕ = 135 deg, X_{LE} = 0.45, Z = 0.01).

Although the predicted shock-wave position was correct, the pressure magnitude predictions were based only on the free-stream flow crossing an assumed two-dimensional shock wave (i.e., the method ignored the reflection shock at the stationary model surface) and the pressure magnitude match may have been coincidental.

The unsteady effects associated with the initial shock wave at transducer positions located off the plate centerline (ϕ = 30 and 60 deg) were more difficult to assess because of the influence of the flow expansion that occurred about the wedge-store edge. However, when the shock-wave passing occurred at separation distances greater than half of a wedge width (i.e., the

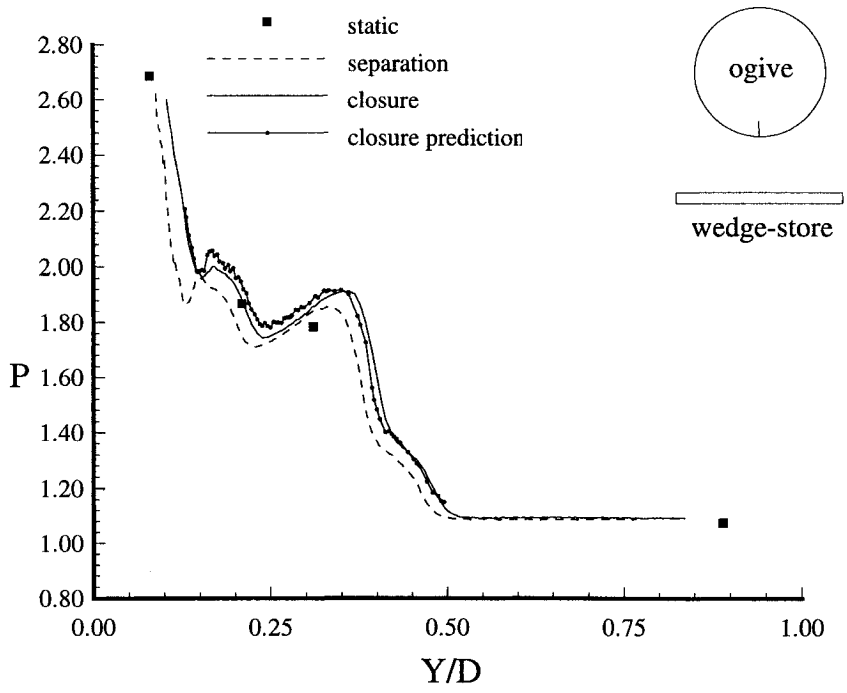

Fig. 15 Ogive surface pressure at X/YE = 2.57 and ψ = 0 deg (6.1 deg, M = 1.9).

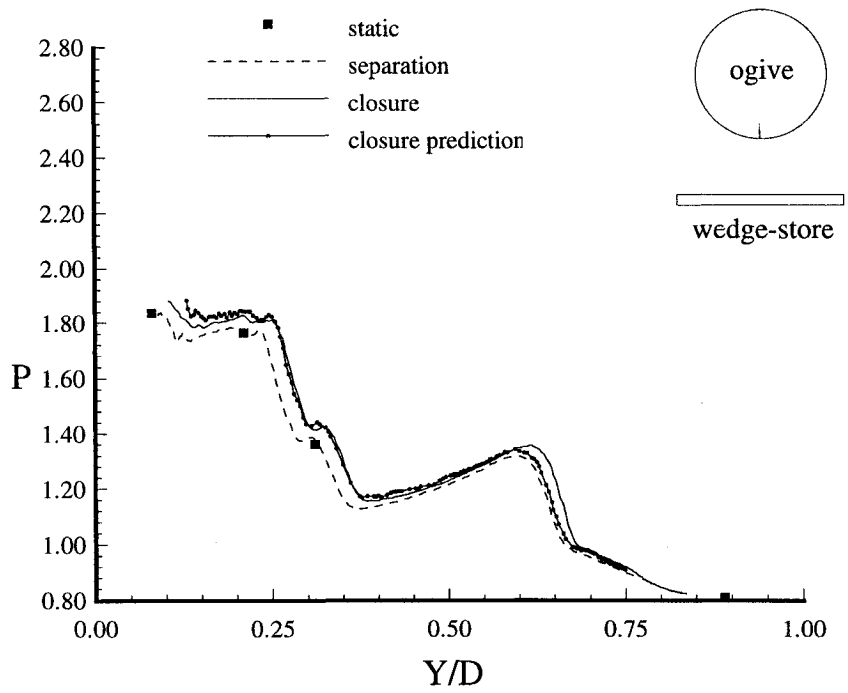

Fig. 16 Ogive surface pressure at X/YE = 3.64 and ψ = 0 deg (6.1 deg, M = 1.9).

initial shock-induced pressure peak was found at $Y/D > 0.50$), the prediction method matched the magnitude of the closure event pressure profile. An example is given in Fig. 9. Although the results of the prediction method could not assess the possibility of off-centerline shock wave unsteadiness, the experimental results did show that any shock-induced unsteadiness would be small.

In the near-touch phase, however, the unsteady effects cannot be ruled out. As seen in Fig. 14, the region of plate surface pressures free of direct shock-wave influences were significantly higher for the closure event than for the separation event. The largest pressure difference found during the near-touch phase (X_{LE} = 0.45, Z = 0.01) was $\Delta P \approx 0.12$, and it was approximately four times greater than the piston theory correction. Though the surface pressures were similar to the responses found in a two-dimensional piston action,[16] the experimental closure pressure exceeded the predicted pressure magnitude of the piston theory because of several factors. First, although the flowfield about the wedge store and plate during the near-touch phase of separation is a complicated three-dimensional flow, predicted surface pressures were based on a simplified two-dimensional analytical theory. Second, the boundary-layer on the plate increases downstream of the coalescing shock waves during the near-touch phase of separation. This thick boundary layer is not accounted for in inviscid flow assumptions, and additionally, the boundary layer may allow an upstream pressure propagation.

Ogive Configuration

Again, the closure event was predicted using steady-state assumptions to assess the possibility of an unsteady shock-wave development. In the ogive and wedge-store separation event an oblique–conical shock-wave interaction is a possible source of unsteadiness. The effective angle correction for the initial attached shock wave in the wedge store and ogive configuration was only made along the symmetry plane from the wedge vertex to the oblique–conical shock-wave intersection. Downstream of the oblique–conical shock-wave intersection, the refracted oblique shock wave was assumed to propagate along a straight path to the ogive surface. Where the wedge store and ogive were close together ($Y/D < 0.60$), the distance from the oblique–conical intersection was small, and the straight shock-wave assumption was reasonable within the conical flow. A closure event prediction is shown for $X/YE = 2.57$ with $\psi = 0$ deg (Fig. 15), where the initial shock-induced pressure peak occurred at $Y/D = 0.36$. However, the two-dimensional planar shock-wave assumption within the conical flow becomes unreliable at greater separation distances as the oblique shock wave begins to curve. For example, the initial shock-induced pressure peak in the closure event was underpredicted, as seen in Fig. 16 near $Y/D = 0.62$.

As discussed earlier, an increase in ψ resulted in a reduction in the magnitude of the shock-induced pressure rise. At forward transducer positions, $X/YE \leq 3.33$ and $\psi > 0$ deg, the α_e prediction method overpredicted the pressure, as there was little difference between the time-dependent events. However, downstream on the cylindrical portion of the model, $X/YE > 3.33$, where the flow deflection across the shock impingement was similar in magnitude to the flow deflection at the oblique–conical shock interaction, the prediction method approximated the initial shock-induced pressure influence.

Conclusions

The evaluation of transient effects and the use of steady-state assumptions were made by comparing the shock-wave-induced pressure profiles of the steady-state, time-dependent, and prediction results of wedge-store separation events. The uncorrected surface pressure vs separation distance showed that the steady-state surface pressure of the stationary model compared favorably with the surface pressures induced during the time-dependent separations. The small differences between the pressure profiles follow the expected trend in shock-wave-induced magnitude and separation position caused by the known differences in the effective wedge angle α_e. Furthermore, the agreement between the steady-state and time-dependent events for the major characteristics of the pressure profile points to the conclusion that the time-dependent motion of the wedge store does not significantly affect the shock waves developing between the two bodies.

Since it was not possible to experimentally achieve time-dependent separation events having equivalent effective AOAs while at the same time having different induced AOAs (as in Belk's numerical study[7]), the transient effects had to be determined indirectly using steady-state assumptions to perturb a selected time-dependent database to predict a second time-dependent event that differed in α_e and direction of the wedge-store motion. This prediction method matched the time-dependent closure event along the plate centerline ($\phi = 0$ deg). Predictions were also favorable within the configuration symmetry plane on the stationary ogive surface ($\psi = 0$ deg) for separation distances less than 60% of the wedge width. The result of the prediction method matching the closure event indicates that within the configuration symmetry plane the steady-state assumptions are valid, and that there are no significant unsteady effects associated with the initial shock wave attached to a moving store.

Surface pressure predictions for locations off the plate centerline ($\phi \neq 0$ deg) were more difficult to accomplish because of the curving initial attached shock wave and the limitations of the two-dimensional prediction method. However, as the distance from the configuration symmetry plane increased, the pressure differences caused by the changes in the effective wedge angle α_e decreased; therefore, any unsteady effects that may exist outside the configuration symmetry plane are small.

In the near-touch phase of separation where body interference dominates the flow (separation distances less than 20% of the store width), and in the region free of the shock-wave influence, there are indications that the time-dependent effects are significant. The surface pressures on the plate and ogive were greater during the closure event than for the separation event, and the pressure characteristics were similar to the responses found in a piston action. However, the experimental pressure differences between the two time-dependent events exceeded the magnitude of the piston theory predictions. The discrepancy between experiment and theory is caused by, in part, the theory assumptions not accounting for a thick boundary layer. This boundary layer contradicts the Newtonian assumptions and provides a mechanism for an upstream pressure propagation.

Finding no significant unsteady pressure effects associated with the initial shock wave gives preliminary support for the quasisteady wind-tunnel methods currently used in store separation predictions. The captive trajectory support and the grid survey wind-tunnel techniques, which position the store at a steady-state attitude that includes an estimated induced angle, will simulate the appropriate time-dependent flowfield with respect to a secondary stationary model. However, unsteady surface pressure cannot be ruled out for small separation distances.

The unsteady piston effects are exacerbated when semi-two-dimensional bodies are separated from the tangent position, such as was simulated by the plate and wedge-store configuration. Thus, aircraft configured with conformal or tangent carriages combined with angular-shaped stores (flat surface adjacent to aircraft) will be more susceptible to the unsteady piston effects. These desired aircraft and store configurations that are designed to reduce drag and radar signature are inherently more difficult to separate, and therefore, trajectory predictions become more complicated. The unsteady piston effect during a time-dependent store separation event will differ from the measured steady-state wind-tunnel results. Although the unsteady piston effect has been identified experimentally, future studies will be required to address how time-dependency information can be integrated into the initial conditions of appropriate store trajectory prediction methods.

Acknowledgments

The authors thank the U.S. Air Force Office of Scientific Research for funding the model fabrication. They also thank the U.S. Air Force Institute of Technology model shop, the Trisonic Gasdynamic Facility test crew, and Russel Osborn of Wright Laboratory/Flight Dynamics Directorate, for their expertise and wind-tunnel support.

References

[1]Mendenhall, M. R. (ed.), "Missile Aerodynamics Panel," *NEAR Conference on Missile Aerodynamics*, Paper 15, 1988, p. 2.

[2]Wood, M. E., "Application of Experimental Techniques to Store Release Problems," *NEAR Conference on Missile Aerodynamics*, Paper 5, 1988, pp. 33–35.

[3]Dougherty, F. C., Benek, J. A., and Steger, J. L., "On Applications of Chimera Grid Schemes to Store Separation," NASA TM 88193, Oct. 1985.

[4]Dougherty, F. C., and Kuan, J.-H., "Transonic Store Separation Using a Three-Dimensional Chimera Grid Scheme," AIAA Paper 89-067, Jan. 1989.

[5]Dougherty, F. C., and Kuan, J.-H., "Computational Store Separation Simulation," *Store Carriage, Integration and Release*, The Royal Aeronautical Society, April 1990, pp. 27.1–27.13.

[6]Meakin, R. L., and Suhs, N. E., "Unsteady Aerodynamic Simulation of Multiple Bodies in Relative Motion," AIAA Paper 89-1996, 1989.

[7]Belk, D. M., Janus, J. M., and Whitfield, D. L., "Three-Dimensional Unsteady Euler Equations Solutions on Dynamic Grids," AIAA Paper 85-1704, July 1985.

[8]Meakin, R. L., "Transient Flow Field Responses About the Space Shuttle Vehicle During Ascent and SRB Separation," *Store Carriage, Integration and Release*, The Royal Aeronautical Society, April 1990, pp. 29.1–29.16.

[9]Pai, S. I., "On the Flow Behind an Attached Curved Shock," *Journal of the Aeronautical Sciences*, Vol. 19, Nov. 1952, pp. 734–742.

[10]Clark, G. F., "Trisonic Gasdynamic Facility User Manual," U.S. Air Force Wright Aeronautical Labs. TM-82-176-FIMM, April 1982.

[11]Press, W. H., Flannery, B. P., Teukolsky, S. A., and Vettering, W. T., *Numerical Recipes: The Art of Scientific Computing*, Cambridge Univ. Press, New York, 1989, pp. 455, 456.

[12]Mosbarger, N. A., "An Experimental Investigation of the Time-Dependent Separation of Tangent Bodies in Supersonic Flow," Ph.D. Dissertation, U.S. Air Force Inst. of Technology, Wright–Patterson AFB, OH, 1994.

[13]Kuethe, A. M., and Chow, C. Y., *Foundations of Aerodynamics: Bases of Aerodynamic Design*, 3rd ed., Wiley, New York, 1976, p. 233.

[14]Arnold, R. J., and Epstein, C. S., "Store Separation Flight Testing," pp. 2, AGARD, AG-300, Vol. 5, April 1986.

[15]Yin, X. Z., and Aihara, Y., "A Method for Calculating Three-Dimensional Shock Interaction (Part 1) Regular Case," *Transactions of the Japan Society for Aeronautical and Space Sciences*, Vol. 33, No. 100, 1990, pp. 55–65.

[16]Heaslet, M. A., and Lomax, H., "Two-Dimensional Unsteady Lift Problems in Supersonic Flight," NACA Rept. 945, 1949, p. 472.